Available online at www.sciencedirect.com
ScienceDirect
Acta Materialia 58 (2010) 1097–1103
Acta MATERIALIA
www.elsevier.com/locate/actamat

Nonpolar ZnO film growth and mechanism for anisotropic in-plane strain relaxation

P. Pant [a,*], J.D. Budai [b], J. Narayan [a]

[a] Department of Materials Science and Engineering, EB-I, Centennial Campus, North Carolina State University, Raleigh, NC 27695-7907, USA
[b] Materials Science and Technology Division, Oak Ridge National Laboratory, Oak Ridge, TN 37831-6030, USA

Received 17 August 2009; accepted 19 October 2009
Available online 26 November 2009

Abstract

Using high-resolution transmission electron microscopy (HRTEM) and X-ray diffraction, we investigated the strain relaxation mechanisms for nonpolar (1 1 −2 0) *a*-plane ZnO epitaxy on (1 −1 0 2) *r*-plane sapphire, where the in-plane misfit ranges from −1.5% for the [0 0 0 1]ZnO||[1 −1 0 −1]sapphire to −18.3% for the [−1 1 0 0]ZnO||[−1 −1 2 0]sapphire direction. For the large misfit [−1 1 0 0]ZnO direction the misfit strains are fully relaxed at the growth temperature, and only thermal misfit and defect strains, which cannot be relaxed fully by slip dislocations, remain on cooling. For the small misfit direction, lattice misfit is not fully relaxed at the growth temperature. As a result, additive unrelaxed lattice and thermal misfit and defect strains contribute to the measured strain. Our X-ray diffraction measurements of lattice parameters show that the anisotropic in-plane biaxial strain leads to a distortion of the hexagonal symmetry of the ZnO basal plane. Based on the anisotropic strain relaxation observed along the orthogonal in-plane [−1 1 0 0] and [0 0 0 1]ZnO stress directions and our HRTEM investigations of the interface, we show that the plastic relaxation occurring in the small misfit direction [0 0 0 1]ZnO by dislocation nucleation is incomplete. These results are consistent with the domain-matching paradigm of a complete strain relaxation for large misfits and a difficulty in relaxing the film strain for small misfits.
© 2009 Acta Materialia Inc. Published by Elsevier Ltd. All rights reserved.

Keywords: Epitaxy; Nonpolar; Anisotropic strain; X-ray; TEM

1. Introduction

Growth of ZnO heterostructures is of significant technological importance because of its optoelectronic applications as light-emitting diodes (LEDs) in the blue and ultraviolet regions of the spectrum [1–3]. Due to its wurtzite structure, film growth along the [0 0 0 1] direction suffers from spontaneous polarization and strain-induced piezoelectric polarization. The polar nature of the [0 0 0 1] axis in wurtzite structures leads to the spontaneous formation of large sheet charges at the interfaces which lowers the electron–hole recombination probability and consequently photon generation efficiency of LEDs. In addition, the residual strain contributes to strain-induced piezoelectric polarization, which can generate internal fields and lower the photon generation efficiency of LEDs further. The residual strain in thin films consists of three components: (i) lattice misfit strain; (ii) thermal misfit strain; and (iii) defect strain. The generation of large electrostatic fields due to spontaneous and piezoelectric strain in thin film structures reduces the overlap between the electron and hole wave functions in quantum well structures and consequently lowers the internal quantum efficiency of LEDs [4]. The polarization effects can be eliminated in epitaxial thin films grown in nonpolar orientations because in these cases the spontaneous component of polarization does not exist and the growth planes consist of both cations and anions. However, residual strain will introduce piezoelectric polarization. Compared to polar ZnO films, which experience isotropic biaxial strain (in-plane) on a *c*-plane sapphire substrate, the biaxial in-plane strain for nonpolar ZnO films is

* Corresponding author. Tel.: +1 919 515 7219; fax: +1 919 515 7724.
E-mail address: ppant@ncsu.edu (P. Pant).

1359-6454/$36.00 © 2009 Acta Materialia Inc. Published by Elsevier Ltd. All rights reserved.
doi:10.1016/j.actamat.2009.10.026

anisotropic due to the anisotropies in the lattice misfit as well as in the thermal expansion coefficients of the film and the substrate in the in-plane directions. The presence of strain is known to affect the electronic band structure and the optical response of semiconductor materials [5]. In the case of nonpolar *a*-plane ZnO films grown on r-sapphire, the presence of an in-plane anisotropy of optical characteristics has been reported [6]. The anisotropic strain in nonpolar ZnO heterostructures can be applied to optical switching and polarization sensitive photodetectors, as has been demonstrated in the case of GaN thin-film heterostructure devices [7,8].

Heteropitaxial growth of nonpolar *a*-plane ZnO has been reported on *r*-plane sapphire [9–11]. Chauveau et al. [12] used high-resolution transmission electron microscopy (HRTEM) to qualitatively investigate strain relaxation in molecular beam epitaxy (MBE)-grown thick films (~1 μm). Their results showed that there is almost a complete strain relaxation along the large misfit [−1 1 0 0]ZnO direction, whereas the strain relaxation along the small misfit [0 0 0 1]ZnO direction is incomplete. They explained their results using the paradigm of domain-matching epitaxy (DME) [13], which predicts growth characteristics of fully relaxed films for large misfits (>7%) and difficulty in strain relaxation for the case of small lattice misfits. Saraf et al. [14] used X-ray diffraction to study strain relaxation in metal–organic chemical vapor deposition (MOCVD)-grown films, and reported strain values of 0.4% along [1 −1 0 0]ZnO, −0.6% along [0 0 0 1]ZnO and 0.3% along [1 1−2 0]ZnO for films ~250 nm thick and strain values of 0.25% along [1 −1 0 0]ZnO, 0.47% along [0 0 0 1]ZnO and 0.15% along [1 1 −2 0]ZnO for films 520 nm thick. In both of these cases, details of thin-film epitaxy and strain relaxation mechanisms were not discussed in detail. In the present work, we have combined high-resolution X-ray diffraction with HRTEM to investigate the details of misfit strain relaxation, where the total strain consists of lattice misfit, thermal misfit and defect strain. We observed relaxation in relatively thinner (~175 nm thick) films with measured strain values of 0.17% along [−1 1 0 0]ZnO, −0.4% along [0 0 0 1]ZnO and 0.04% along [1 1 −2 0]ZnO. A comparison of the reported strain in the films by different growth processes [12,14] and our work shows that, by the pulsed laser deposition (PLD) growth process, we were able to relax the strain in the films at much smaller values of film thickness. This is because the PLD growth technique is a highly energetic process compared to MBE and MOCVD, and the kinetic energies of the ablated species in PLD lie in a range that promotes surface mobility of the atoms at the surface to enable their migration to thermodynamically stable sites.

In our previous work [15], we reported the structure property correlations of (1 1 −2 0) *a*-plane ZnO films grown on (1 −1 0 2) *r*-plane sapphire substrate. In the present work, we report a comprehensive study of the strain anisotropy in (1 1 −2 0)ZnO films grown on (1 −1 0 2)sapphire substrate, based on determination of in-plane and out-of-plane lattice parameters, generation of misfit dislocations at the interface and plastic strain relaxation in the film by dislocation nucleation due to activation of slip systems for nonpolar wurtzite film growth. Our detailed X-ray measurements show that the presence of anisotropic in-plane strain causes a distortion of the hexagonal symmetry of the basal plane. The symmetry distortion is explained by the fact that the strains in the basal plane are not isotropic along [−1 1 0 0]ZnO and [1 1 −2 0]ZnO. This is because ZnO is stress free in the [1 1 −2 0]ZnO growth direction, whereas it is under stress by the substrate along the [−1 1 0 0]ZnO direction. Our results show that there is almost a complete relaxation of strain in the large misfit [−1 1 0 0]ZnO direction, whereas it is difficult to relax the strain in the small misfit [0 0 0 1]ZnO direction. Lattice relaxation by dislocations is facilitated either by misfit dislocations at the interface or by dislocation nucleation at the free surface and propagation to the interface. Dislocation nucleation at the free surface is limited by the free surface step energy and the lattice misfit strain, whereas dislocation propagation is controlled by the lattice frictional stress. It is argued that for a small misfit, where critical thickness is large, both dislocation nucleation and glide steps provide barrier to a full relaxation.

2. Experimental

The ~175 nm thick (1 1 −2 0)ZnO films were grown by pulsed laser deposition at 500 °C on (1−1 0 2)sapphire substrates by focusing a KrF excimer laser with a wavelength of 248 nm and a pulse duration of 25 ns on a ZnO target. The energy density of the laser beam was 2–3 J cm^{-2} with a repetition rate of 5 Hz. Our method resulted in the formation of high-quality thin films at the relative low temperature of 500 °C. The base pressure of the chamber prior to deposition was 7E−7 Torr and deposition was carried out at an oxygen partial pressure of 2E−4 Torr. The X-ray scans of the films were measured on a Huber 4-circle diffractometer with a vertically focusing graphite (0 0 0 2) monochromator before the sample and Soller slits after the sample. The instrumental resolution was determined to be 0.075°. A JEOL 2010F electron microscope operating at 200 kV with a point-to-point resolution of 1.8Å and STEM-Z resolution of 1.2 Å with a Gatan image filter attachment was used for determination of the nature of the dislocation and strain relaxation of the film, and to establish the detailed epitaxial relationship between the film and the substrate.

3. Results and discussion

Fig. 1 shows X-ray diffraction ϕ-scans through the ZnO(1 0 −1 0) and *c*-axis Al_2O_3(0 0 0 12) reflections. The epitaxial relationship between the film and the substrate was determined by 2θ-ω scans and ϕ-scans to be (1 1 −2 0)ZnO‖(1 −1 0 2)sapphire, [0 0 0 1]ZnO‖[1 −1 0 −1] sapphire and [−1 1 0 0]ZnO‖[−1 −1 2 0]sapphire. The *L*-scans through the (1 0 −1 *L*) peaks in reciprocal space

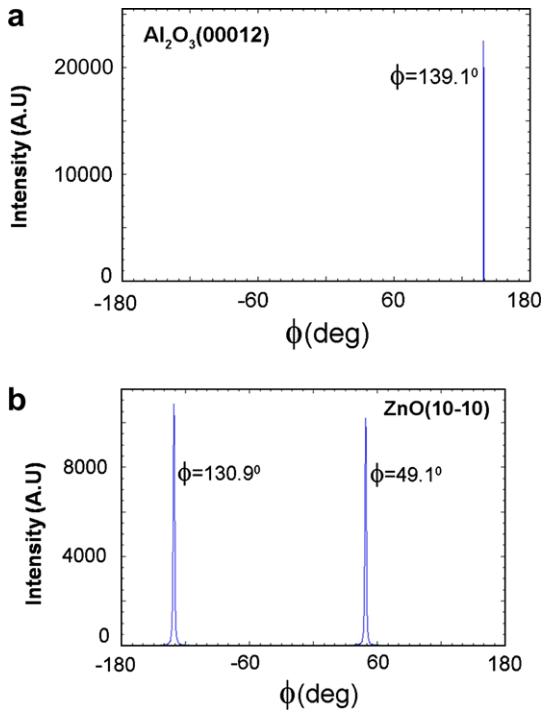

Fig. 1. ϕ-scan through Al_2O_3(0 0 0 1 2) and through ZnO(1 0 −1 0) showing the in-plane orientation of the sapphire substrate and the film.

which probe the stacking sequence (wurtzite (ababab) vs. zincblende (abcabcabc)) in a crystal structure were used to verify the presence of only the wurtzite phase of ZnO in the films. The L-scan in Fig. 2 shows peaks only at integral positions, thereby confirming the wurtzite structure of the film. A schematic of the epitaxial relationship between (1 1 −2 0)ZnO films on (1 −1 0 2)sapphire substrate is shown in Fig. 3a. The calculated value of the room temperature lattice mismatch along the in-plane ZnO[0 0 0 1] is only −1.5%, while the lattice mismatch along the in-plane ZnO[−1 1 0 0] is −18.3%. The observed in-plane epitaxial relationship with a small misfit along the c-axis of ZnO and a large misfit along the m-axis of ZnO can be explained by the paradigm of domain-matching epitaxy [13,15], where matching of domains of lattice planes is considered

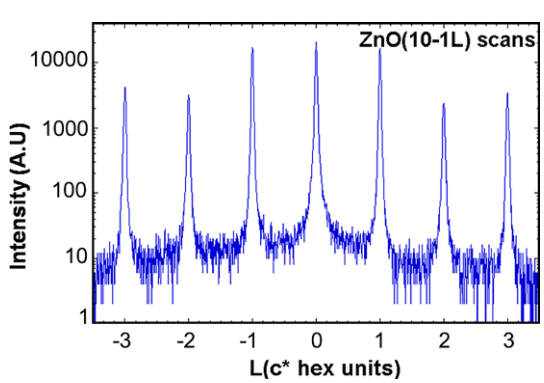

Fig. 2. ZnO(1 0 −1 L) scan with peaks only at integral values, verifying the wurtzite structure of ZnO film.

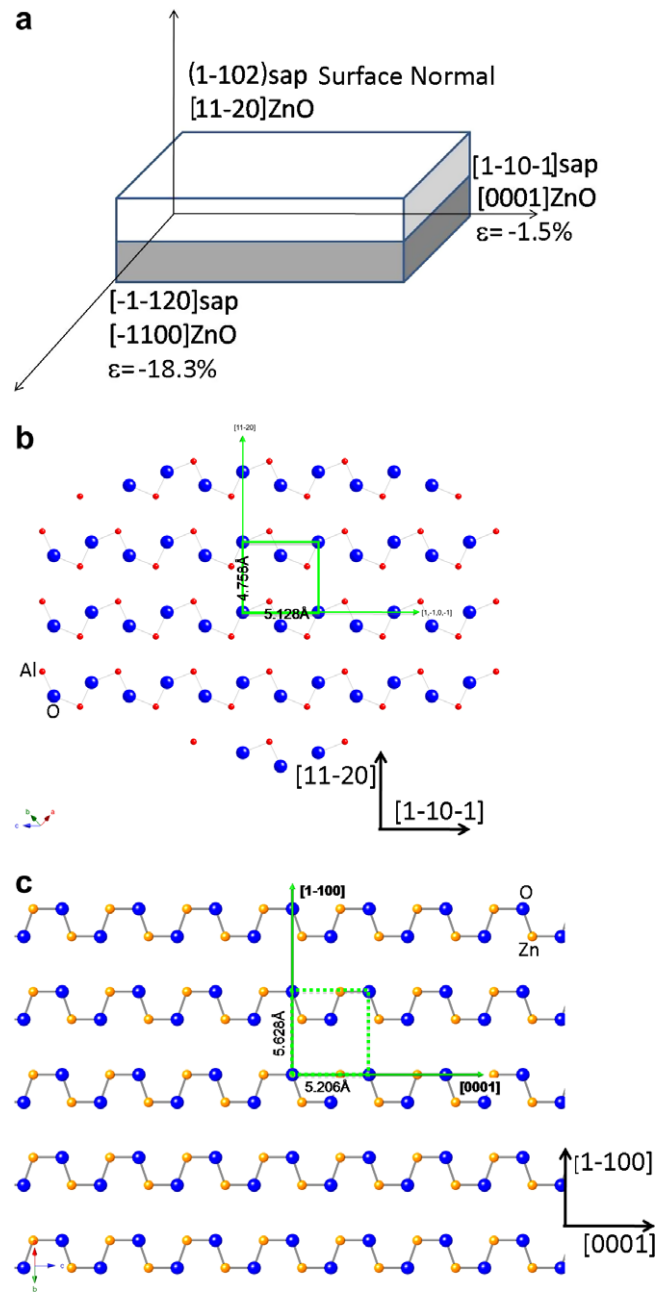

Fig. 3. (a) A schematic showing the epitaxial relationship between a-plane ZnO films grown on r-plane sapphire. Schematics of the top surface of (b) (1 −1 0 2)sapphire and (c) (1 1 −2 0)ZnO respectively.

along the film–substrate interface. Fig. 3b and c shows schematics of the top views for r-plane (1 −1 0 2)sapphire and a-plane (1 1 −2 0)ZnO, where only single atom planes of each species are included. The surface unit cells for ZnO and sapphire have been labeled in the projected images. The in-plane translational period of ZnO along [1 −1 0 0]ZnO is 5.628 Å, while the translational period for [1 1 −2 0]Al_2O_3 is 4.758 Å, which gives a lattice misfit of −18.3% along [1 −1 0 0]ZnO. The large misfit of −18.3% along [1 −1 0 0]ZnO can be accommodated by matching of two alternating domains of lattice planes. In one domain five ZnO(1 −1 0 0) planes match six sap-

phire(1 1 −2 0) planes. In the other domain, six ZnO(1 −1 0 0) planes match with seven sapphire(1 1 −2 0) planes. The misfit will be completely relaxed if these domains alternate with a frequency of 3:2. The translational period along [0 0 0 1]ZnO is 5.206 Å and the translational period along [1 −1 0 −1]Al_2O_3 is 15.384 Å. The [1 −1 0 −1]Al_2O_3 translational period is approximately three times that of [0 0 0 1]ZnO, which gives a lattice misfit of −1.5% along [0 0 0 1]ZnO.

An HRTEM micrograph from the film–substrate interface region taken along the [1 −1 0 −1] zone axis of ZnO is shown in Fig. 4a. The HRTEM micrograph of the interface region clearly delineates an atomically sharp and abrupt interface with no interfacial reaction, as shown in Fig. 4b. Along [0 0 0 1]ZnO the lattice misfit is −1.5%, but the net residual strain is −0.4%, which is relaxed by the generation of a dislocation whose spacing is given by $|b|/\varepsilon_{rr}$, corresponding to a full relaxation, where ε_{rr} is the relaxed component of the strain. Thus, we expect to see only dislocations separated by a relatively large distance. Fig. 4a shows a dislocation in the field of view with a missing plane in ZnO, which is consistent with the net residual strain being compressive (negative) in the small misfit direction. The Burgers circuit for the dislocation is illustrated in Fig. 4a. The points marked *S* and *F* indicate the "start" and "finish" of the circuit. The dislocation is identified as belonging to the slip system {0 −1 1 1}⟨1 1 −2 3⟩. It can be clearly seen that the dislocation which starts from the surface does not reach the interface. The dislocation termination in the film explains the residual compressive strain measured in the small misfit direction. This is consistent with the stress relaxation mechanism discussed later.

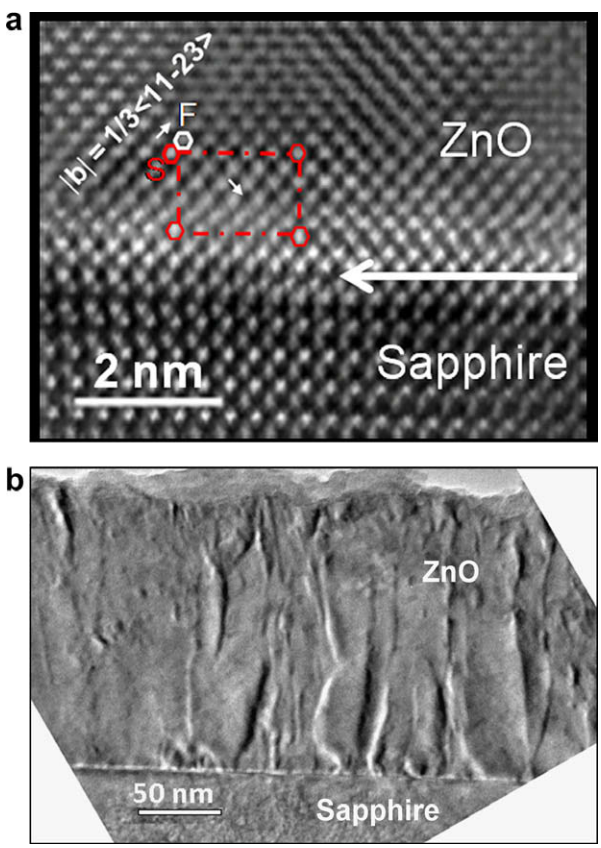

Fig. 4. (a) HRTEM micrograph taken along the [1 −1 0 −1] zone axis of ZnO showing a dislocation with a missing plane in ZnO which is consistent with the net residual strain being compressive. The points marked *S* and *F* indicate the "start" and "finish" of the Burgers circuit for the dislocation. The dislocation is identified as belonging to the slip system (0 1 −1 −1) ⟨1 1 −2 3⟩ with a Burgers vector of 1/3 ⟨1 1 −2 3⟩. (b) Low-magnification image of the interface.

To determine the lattice parameters along the three principal directions shown in Fig. 3a, the *d*-spacings for (*h k i l*) planes in different directions were measured. High-resolution X-ray 2θ-ω scans were used to determine the *d*-spacings. The *d*-spacings of the (1 1 −2 0) and (1 −1 0 0)ZnO planes do not depend on the *c* lattice parameter, but, due to anisotropic strain, they are expected to reveal slightly different values for the effective *a* lattice parameter. The (1 1 −2 0) *d*-spacing was measured directly to determine the out-of-plane ZnO *a* lattice parameter. The (1 −1 0 0) ZnO planes are at $\psi = 90°$ from the surface normal (1 1 −2 0)ZnO planes and would require difficult X-ray measurements in the in-plane glancing angle geometry. Therefore to determine the *d*-spacing for the (1 −1 0 0) planes the $\sin^2\psi$ technique was used. In this technique, the *d*-spacing was measured for different diffraction peaks in the $l = 0$ plane and as a function of the angle ψ away from the surface normal. To compare the results for different reflections, the *d*-spacings were converted to an effective ZnO lattice parameter *a*. By plotting *a* as a function of the angle away from the surface normal, we obtained both the out-of-plane and the in-plane (by extrapolation) lattice parameters. This type of approach is referred to as a $\sin^2\psi$ technique because a straight line will be obtained when the lattice parameter is plotted as a function of $\sin^2\psi$. Thus *a* at $\sin^2\psi = 0$ corresponds to the out-of-plane (normal) ZnO lattice parameter along the [1 1 −2 0] direction and *a* at $\sin^2\psi = 1$ corresponds to the in-plane lattice parameter along the [1 −1 0 0] direction. Fig. 5 is a stereographic projection showing the (1 1 −2 0)ZnO pole and the $l = 0$ reflections used for this measurement (circled in red). The calculated *a* lattice parameters for the different diffraction peaks in the $l = 0$ plane are listed in Table 1. Fig. 6 shows a plot of the ZnO *a* lattice parameter versus $\sin^2\psi$ using peaks in the $l = 0$ plane. By extrapolation of the line, the *a* lattice parameter along [1 −1 0 0] was determined to be 3.2555 Å at $\sin^2\psi = 1$. The in-plane *c* lattice parameter was also measured indirectly since the (0 0 0 1) reflection is also at a glancing angle inclination of 90° from the surface normal. First the *d*-spacing in the $l = 0$ plane (e.g. (1 1 −2 0)ZnO surface normal) was measured and then *c* was calculated from measurements of the *d*-spacing for reflections with some dependence on *c*. To get accuracy in the measurement, several reflections with a large *c*-component were used. These reflections are indicated by the green circles in Fig. 5. These results for *c* lattice parameters are shown in Table 2. The measured value for the in-plane ZnO *c* lattice parameter is 5.186 Å.

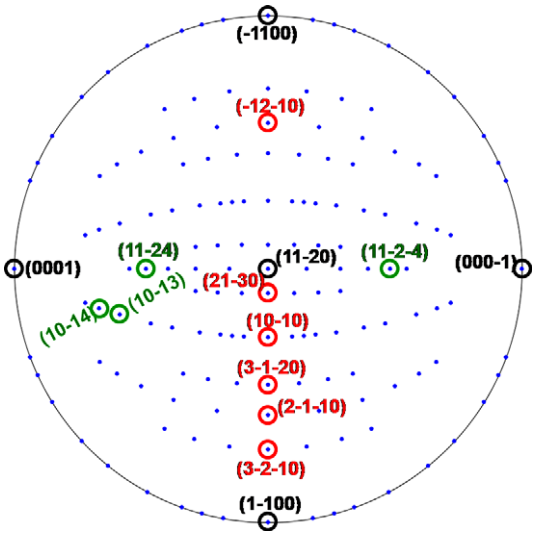

Fig. 5. Stereographic projection of the (1 1 −2 0)ZnO plane. (1 1 −2 0) is the surface normal plane. The red circles show the reflection peaks used to determine the a lattice parameter along [1 −1 0 0]ZnO. The green circles show the reflection peaks used for determination of the c lattice parameter. (For interpretation of the references to colour in this figure legend, the reader is referred to the web version of this article.)

Table 1
Measured values of a lattice parameter of the (h k i l) planes with $l = 0$ as a function of the angle away from the surface normal.

ZnO(h k i l)	$\psi = 90°$-chi	$\sin^2\psi$	d-spacing	a (Å)
(1 1 −2 0)	0.00	0.0000	1.6256	3.2512
(1 1 −2 0)	0.00	0.0000	1.6256	3.2513
(2 1 −3 0)	10.9	0.0358	1.0640	3.2506
(1 0 −1 0)	30.0	0.2500	2.8165	3.2522
(2 0 −2 0)	30.0	0.2500	1.4083	3.2524
(3 −1 −2 0)	49.1	0.5720	1.0648	3.2530
(2 −1 −1 0)	60.0	0.7500	1.6273	3.2546
(−1 2 −1 0)	60.0	0.7500	1.6273	3.2547
(3 −2 −1 0)	70.9	0.8929	1.0653	3.2548

Table 3 lists the measured and bulk literature values of the lattice parameters along the three epitaxial directions. From the tabulated values we can make the following conclusions. First, the measured value of the lattice parameter $a = 3.251$ Å along the [1 1 −2 0]ZnO direction that is the surface normal ($\psi = 0°$) shows that the out-of-plane film response to in-plane stresses is tensile, with a residual strain of +0.04%. Second, the in-plane [−1 1 0 0]ZnO direction shows a measured residual strain of +0.17% vis-à-vis the calculated misfit of −18.3%. The calculated thermal contraction strain for growth at 500 °C in [−1 1 0 0]ZnO is negligibly small at 0.01%. This indicates that the misfit strain is completely relaxed in the large misfit direction and the observed strain could be explained mainly by the presence of defects since the thermal strain along this direction is negligibly small. It is interesting to note here that along [1 1 0 0]ZnO a final, small tensile strain results from a large compressive lattice mismatch. Third, in the [0 0 0 1]ZnO direction, the measured value of c is 5.186 Å

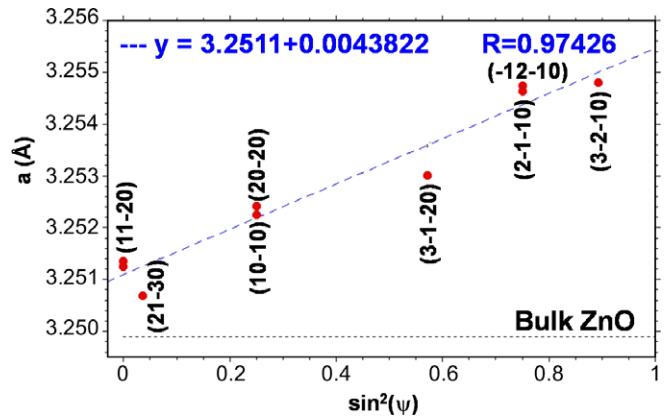

Fig. 6. Plot of a lattice parameter as a function of $\sin^2\psi$ (ψ angle of the diffraction plane normal away from the surface normal) for $l = 0$ planes. Extrapolation of the plot at $\sin^2\psi = 1$ was used to determine the value of a along [1 −1 0 0].

indicating the presence of a residual strain of −0.4% vs. the initial lattice misfit of −1.5%. The calculated thermal strain along this direction is −0.18%. These values suggest that strain relaxation along the in-plane [0 0 0 1]ZnO direction is more difficult and does not occur at the same rate as along the [−1 1 0 0]ZnO direction.

The strain in thin films generally has three components: (i) lattice misfit strain; (ii) thermal differential contraction strain; and (iii) defect strain. The defect strain is related to the inherent defect (point defects) strain associated with the growth ambient of ZnO films and the dislocations strain. For the growth of nonpolar (1 1 −2 0)ZnO films we can conceptually think of the tetrahedrally coordinated ZnO structure with a hexagonal lattice to be distorted by different substrate-induced in-plane stresses along the two orthogonal in-plane directions [0 0 0 1]ZnO and [−1 1 0 0]ZnO. The growth of the [1 1 −2 0]ZnO structure can thus be described as a triaxially strained hexagonal lattice, where strains in the two different in-plane directions are controlled by the anisotropic lattice matching and thermal contraction of the film and the substrate. The out-of-plane lattice parameter is determined by an anisotropic Poisson's ratio effect. If we consider the natural coordinate system xyz, in which the natural coordinate z is in direction [0 0 0 1] of the wurtzite crystal lattice and the x and y coordinates are in the basal (0 0 0 1) plane, then the isotropy of the basal plane allows us to select the x-axis along [1 1 −2 0]ZnO and the y-axis along [−1 1 0 0]ZnO (orthogonal directions in the basal plane). Considering the relation between the stress σ and strain ε tensors in linear elasticity

Table 2
ZnO reflections used to measure the c lattice parameter.

ZnO(h k i l)	$\psi = 90$-chi	c (Å)
(1 1 −2 4)	51.3	5.1862
(1 1 −2 −4)	51.3	5.1865
(1 0 −1 3)	63.0	5.1864
(1 0 −1 4)	68.7	5.1854

Table 3
Bulk literature values of the lattice misfit and the thermal strain in the in-plane directions, [0 0 0 1] and [−1 1 0 0]ZnO respectively, measured values of the lattice parameters in the film and the corresponding residual strain along the surface normal and the in-plane directions.

	Calculated				Experimental (measured)	
	Lattice parameter[a] (Å)	Lattice misfit strain ε_l (%)	α (E−6 K^{-1}) at 873 K[b]	Thermal misfit strain ε_t (%)	Lattice parameter (Å)	Residual strain in film ε (%)
[−1 1 0 0]ZnO	5.6288	−18.3	8.47	0.01	5.6386	0.17
[−1 −1 2 0]sapphire	4.758		8.25			
[0 0 0 1]ZnO	5.2066	−1.5	4.936	−0.18	5.186	−0.4
[−1 1 0 1]sapphire	15.384		8.59			
[11 −2 0]ZnO	3.2498				3.251	0.04

[a] See Ref. [16].
[b] See Ref. [17].

theory, $\sigma_{ij} = C_{ijkl}\varepsilon_{kl}$, where the coefficients C_{ijkl} are the elastic constants, the strain state in the film for growth along [1 1 −2 0]ZnO can be expressed as

$$\varepsilon_{xx} + \frac{C_{12}}{C_{11}}\varepsilon_{yy} = -\frac{C_{13}}{C_{11}}\varepsilon_{zz}$$

where the stress σ_{xx} along the growth direction [1 1 −2 0]ZnO is zero. From the measured strain values in the film listed in Table 3 we can infer that the in-plane strains cause a relaxation of the film in the normal growth direction. The experimentally determined values of the lattice parameters along the growth directions also show that the *a* lattice parameter has different values along the in-plane [−1 1 0 0]ZnO and out-of-plane [1 1 −2 0]ZnO directions, consequent to [1 1 −2 0]ZnO being the stress-free direction. The result of different tensile strains along the [−1 1 0 0]ZnO and [1 1 −2 0]ZnO directions can be visualized as an anisotropic distortion of the ZnO basal plane geometry, a schematic of which is illustrated in Fig. 7.

The lattice misfit along [0 0 0 1]ZnO is −1.5% and the calculated thermal misfit at the growth temperature is −0.18%. Because of the small misfit along [0 0 0 1], it is proposed that film growth occurs pseudomorphically along this direction up to a critical thickness. Since the lattice and thermal misfits are additive, the measured value of −0.4% residual strain shows that the strain is not fully relaxed along [0 0 0 1]ZnO. The measured residual strain of 0.17% along [−1 1 0 0]ZnO compared to an initial large misfit of −18.3% shows that there is a complete relaxation of the lattice misfit along [−1 1 0 0] since the critical thickness under a large misfit (>7%) is typically less than a monolayer. Previous in situ synchrotron X-ray diffraction studies [13] on ZnO/*c*-plane sapphire have shown that the large misfit ∼15.44% can be relaxed within 1–2 monolayers. In view of these results, the relaxation of the lattice misfit along [−1 1 0 0]ZnO can be explained by the integral matching of (1 −1 0 0)ZnO and (1 1 −2 0)sapphire lattice planes and the generation of corresponding geometrical misfit dislocations along the interface [12,13]. Since the thermal strain along this direction is negligibly small, the residual strain can be attributed to the presence of point and microstructural defects in the grown film.

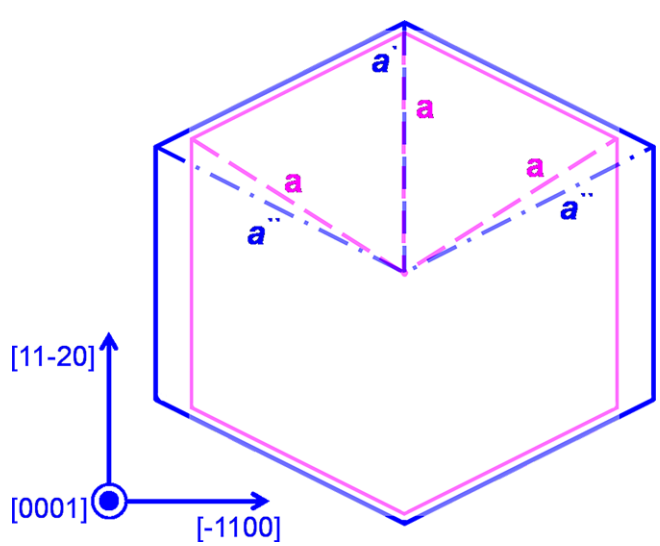

Fig. 7. Distortion of the ZnO basal plane under anisotropic strain for the growth of *a*-plane ZnO on *r*-plane sapphire. —. indicates the undistorted lattice parameter and -·-·-·- indicates the distorted lattice parameter.

Table 4 summarizes the slip systems which can be activated along the two in-plane directions for *a*-plane-oriented nonpolar film growth. Plastic relaxation along [1 −1 0 0]ZnO can be induced by dislocation nucleation due to activation of the {1 0 −1 0}⟨1 −2 1 0⟩ or {0 1 −1 0}⟨1–210⟩ slip systems because of their low energy and high Schmid factors. Also, the high values of the Schmid factors for the pyramidal planes slip systems for stress along the [1 −1 0 0] and [0 0 0 1] directions indicate the possibility of plastic relaxation by activation of these slip systems. The anisotropic strain relaxation observed along the [1 −1 0 0] and [0 0 0 1] stress directions coupled with the fact that the pyramidal plane slip systems can be activated (considering high values of Schmid factors) along these directions suggests that plastic relaxation by dislocation nucleation can be initiated along these directions. The observed strain relaxation suggests that the large misfit stress along [1 −1 0 0]ZnO can promote a complete strain relaxation by generation of misfit dislocations which can be confined in the interface region. On the other hand, the small misfit stress along [0 0 0 1]ZnO is not able to initiate a complete strain relaxation and could explain the residual strain along [0 0 0 1]ZnO. This explanation is

Table 4
Schmid factors for the activated slip systems along the in-plane directions for (1 1 −2 0)ZnO.

	Slip plane	Slip Direction	Schmid factor
Stress direction [1 −1 0 0]			
Prismatic planes	{1 0 −1 0}	⟨1 −2 1 0⟩	0.433
	{0 1 −1 0}	⟨1 −2 1 0⟩	−0.433
Pyramidal planes	{−1 2 −1 2}	⟨−1 2 −1 3⟩	0.337
	{−1 1 0 1}	⟨−1 2 −1 3⟩	0.403
	{0 1 −1 −1}	⟨−2 1 1 0⟩	0.380
Stress direction [0001]			
Pyramidal planes	{1 1 −2 2}	⟨11 −2 3⟩	0.449
	{−1 2 −1 2 }	⟨−1 2 −1 3⟩	0.449
	{−1 1 0 −1}	⟨−1 2 −1 3⟩	0.403
	{0 1 −1 −1}	⟨11 −2 3⟩	0.403

supported by the observation of a dislocation in the HRTEM micrograph in Fig. 4a. The dislocation which represents a missing half plane and hence a compressive strain in the film terminates close to the interface. HRTEM gives information about the projected Burgers vector, and the Burgers circuit gives information about the projection of a dislocation. The dislocation has been identified to lie in the (0 1 −1 −1) plane. From the slip systems associated with *a*-plane ZnO films, for the pyramidal slip system {0 1 −1 −1}⟨2 −1 −1 0⟩ the components of the dislocations will have to be either along [1 1 −2 0]ZnO or [−1 −1 0 0]ZnO directions, i.e. either parallel or perpendicular to the growth plane. The Burgers vector in Fig. 4a is neither parallel nor perpendicular to the growth plane, but is inclined to the interface. Therefore (0 1 −1 −1) {1 1 −2 3} is the slip system likely to be responsible in the present case. The activation of the secondary slip systems observed in hexagonal close-packed (hcp) metals has been explained by the deviation in the ideal hcp *c*/*a* ratio value from 1.633 ($c/a_{\mathrm{ZnO}} = 1.602$) and the slightly different values of the *d*-spacing and normal spacing for the prismatic and pyramidal planes [18].

In summary, we have investigated the anisotropic strain in nonpolar *a*-plane ZnO films grown on *r*-plane sapphire by detailed X-ray diffraction and HRTEM cross-section measurements. The X-ray diffraction measurements of the lattice parameters show that the growth of an [1 1 −2 0]-oriented *a*-ZnO structure can be described as a triaxially strained hexagonal lattice. In this case, the strains in the two different in-plane directions are controlled by the anisotropic lattice matching and thermal contraction of the sapphire substrate, and the out-of-plane lattice parameter is determined by an anisotropic Poisson's ratio. The strained state in the film causes the *a* lattice parameter to have different values along the in-plane [1 −1 0 0] and out-of-plane [1 1 −2 0] directions, which leads to an anisotropic distortion of the ZnO basal plane geometry. Our HRTEM investigations of the interface show that plastic relaxation by dislocation nucleation at the free surface occurring in the small misfit direction is incomplete, which is consistent with measured residual strain along [0 0 0 1] ZnO.

Acknowledgements

The research was supported by the National Science Foundation. The work was also supported by the DOE Office of Science, Division of Material Sciences & Engineering under contract with ORNL, managed by UT-Battelle, LLC.

References

[1] Bagnall DM, Chen YF, Zhu Z, Yao T, Koyama S, Shen MY, et al. Appl Phys Lett 1997;70:2230.
[2] Ryu Y, Lee T-S, Lubguban JA, White HW, Kim B-J, Park Y-S. Appl Phys Lett 2006;88:241108.
[3] Özgür Ü, Alivov YI, Liu C, Teke A, Reshchikov MA, Doğan S, et al. J Appl Phys 2005;98:041301.
[4] Waltereit P, Brandt O, Trampert A, Grahn HT, Menniger J, Ramsteiner M, et al. Nature 2000;406(6798):865.
[5] Hill NA, Waghmare U. Phys Rev B 2000;62:8802.
[6] Nam YS, Lee SW, Baek KS, Chang SK, Song J-H, Han SK, et al. Appl Phys Lett 2008;92:201907.
[7] Ghosh S, Brandt O, Grahn HT, Ploog KH. Appl Phys Lett 2002;81:3380.
[8] Flissikowski T, Omae K, Misra P, Brandt O, Grahn HT. Phys Rev B 2006;74:085323.
[9] Gorla CR, Ematoglu NW, Liang S, Mayo WE, Wraback N, Shen H. J Appl Phys 1999;85:2595.
[10] Mriyama T, Fujita S. Jpn J Appl Phys 2005;44:7919.
[11] Vennéguès P, Chauveau JM, Korytov M, Deparis C, Zuniga-Perez J, Morhain C. J Appl Phys 2008;103:083525.
[12] Chauveau JM, Vennéguès P, Laugt M, Deparis C, Zuniga-Perez J, Morhain C. J Appl Phys 2008;104:073535.
[13] Narayan J, Larson BC. J Appl Phys 2003;93:278.
[14] Saraf G, Lu Y, Siegrist T. Appl Phys Lett 2008;93:041903.
[15] Pant P, Budai JD, Aggarwal R, Narayan RJ, Narayan J. Acta Mater 2009;57:4426.
[16] JCPDS#36-1451,#74-0534,#79-0206 for bulk ZnO, JCPDS # 10-0173 for bulk sapphire.
[17] Toulukian YS, Kirby RK, Taylor RE, Lee TYR. Thermophysical properties of matter, vol 13. Thermal expansion nonmetallic solids. New York: IFI/Plenum, p. 176, 444.
[18] Hirth JP, Lothe J. Theory of dislocations. 2nd ed. New York: John Wiley & Sons Inc.; p. 280–82.